Proceedings of the ASME 2013 Conference on Smart Materials, Adaptive Structures and Intelligent Systems
SMASIS2013
September 16-18, 2013, Snowbird, Utah, USA

SMASIS2013-3070

ADDITIVE MANUFACTURING OF SHAPE MEMORY DEVICES AND PSEUDOELASTIC COMPONENTS

Christoph Haberland **Mohammad Elahinia** **Jason Walker**
Dynamic and Smart Systems Laboratory, University of Toledo, Toledo, Ohio, USA

Horst Meier
Institute Product and Service Engineering, Ruhr University Bochum, Bochum, North Rhine Westphalia, Germany

Jan Frenzel
Institute for Materials, Ruhr University Bochum, Bochum, North Rhine Westphalia, Germany

ABSTRACT

Processing of Nickel-Titanium shape memory alloys (NiTi) is by no means easy because all processing steps can strongly affect the properties of the material. Hence, near-net-shaping technologies are very attractive for processing NiTi due to reduction of the processing route. Additive Manufacturing (AM) provides especially promising alternatives to conventional processing because it offers unparalleled freedom of design. In the last 5 years AM of NiTi received little attention from academics and researchers and, therefore, is far from being established for processing NiTi today. This work is to highlight the current state of the art of using the AM technique Selective Laser Melting (SLM) for processing high quality NiTi parts. For this reason, fundamentals for SLM processing of NiTi are described. It is shown in detail that a careful control of process parameters is of great importance. Furthermore, this work characterizes structural and functional properties like shape recovery, referring to the shape memory effect in Ti-rich SLM NiTi, or pseudoelasticy in Ni-rich SLM NiTi. It is shown that both types of shape memory effects can be adjusted in SLM NiTi by the choice of the raw material and processing strategy. By comparing the properties of SLM NiTi to those of conventionally processed NiTi, this work clearly shows that SLM is an attractive manufacturing method for production of high quality NiTi parts.

INTRODUCTION

Generally, processing of NiTi is challenging [1-5] because the structural and functional properties of this material are significantly influenced, and often degraded, by the processing itself or by (subsequent) heat treatment procedures due to the high reactivity of the alloy [6-8]. On top of this, stress induced martensite, work hardening, spring back effects, burr formation and adhesion can make precise machining quite difficult and can account for significant tool wear [9-11]. For these reasons, most of today's NiTi applications are based on simple geometries (e.g. bar, rod, wire, sheet, tube) due to the lack of processing capabilities. These issues might even limit the use of NiTi for special engineering applications or MEMS because there are competitive yet simpler technologies [12]. Additionally, parts, devices or components made of NiTi are regarded as being comparatively expensive because small production runs or even the production of single batches add to the final product [13].

AM seems to provide high potential because the technology allows for the production of complex parts in small batches and for the production of customized single components [14]. Although it is obvious that AM technologies are attractive for manufacturing NiTi products, they are far from being established for processing NiTi. To date, there are not more than twenty journal and conference papers or published conference posters on AM of NiTi [15]. This is even more remarkable since AM offers considerable flexibility in terms of part's geometry and complexity due to a layer based processing principle. Hence, AM can produce complex parts that may be difficult or impossible to fabricate by any other method [16].

Copyright © 2013 by ASME

Downloaded From: http://proceedings.asmedigitalcollection.asme.org/ on 01/31/2016 Terms of Use: http://www.asme.org/about-asme/terms-of-use

Furthermore, AM may open up completely new perspectives and scopes for design of shape memory applications because filigree and complex three dimensional parts can be produced which cannot be obtained by any other method.

In previous works [15, 17-21], we demonstrated that pre-alloyed NiTi powders can successfully be processed by SLM, which has become one of the most popular AM techniques. The aim of this work is to highlight the current state of the art of using SLM for processing high quality NiTi parts. Therefore, this work captures some of the most important results and shows that the material properties of SLM NiTi strongly depend on the processing conditions and on the process parameter set-up. A careful control of process parameters is of great importance; hence, guidelines for an optimized set-up are given by this paper. Additionally, this work shows that SLM NiTi exhibits distinct functional properties, such as the shape memory effect or pseudoelasticity. By comparing these functional properties to those of conventionally processed NiTi, this work clearly shows that SLM provides an attractive manufacturing method for production of complex and high quality NiTi devices.

EXPERIMENTAL METHODS

Material

For optimized SLM, the powdered material for processing must meet special requirements. All of the powder materials for this work were gas atomized from high-purity ingot materials. Ingots with different Ni-Ti ratios were purchased from Memry GmbH (weil am Rhein, Germany). Gas atomization was perfomed by TLS Technik GmbH & Co Spezialpulver KG (Bitterfeld, Germany) by using the EIGA method (electrode induction melting gas atomization). This method allows for the production of spherical particles with low impurity contents. After atomization the powder was sieved to include a particle size distribution ranging from 25 to 75 µm. This particle size distribution represents a good compromise of flowability, packing density and impurity contents. Details on NiTi powder characteristics and their suitability for SLM processing are described elsewhere [15].

Processing

All samples were produced with a commercial SLM system of type Realizer SLM 100 (MTT Technologies GmbH, now SLM Solutions GmbH) equipped with a 100 W Ytterbium fibre laser. Each process was carried out under an Argon atmosphere to minimize oxidation. For functional testing, all samples were produced with an optimized set-up of process parameters which was identified in our previous works [15, 18]. As a scanning regime, an alternating x/y-movement of the laser was chosen. Details are described elsewhere [28].

Heat treatments (solution annealing and aging) were performed in a muffle furnace (Linn High Therm LM 312) under constant Argon flow. Parameters and details are described elsewhere [15, 20].

Material's characterization

Material density was determined by the Archimedes principle. Details on this method and the experiments are described elsewhere [15, DIN EN ISO 3369].

Chemical analyses were subcontracted to an external company (Revierlabor GmbH, Essen, Germany). Carbon levels were measured using the combustion flame infrared method, Oxygen and Nitrogen levels were measured using the inert gas fusion method.

The phase transformation behavior of the material was characterized by differential scanning calorimetry (DSC; Netzsch DSC 204 F1 Phoenix). The heating and cooling rate was set at 10 K/min. Further details on the procedure are reported elsewhere [15].

Structural and functional analyses were carried out by compression testing using a tensile-compression test instrument of type Zwick/Roell Z100 with an integrated temperature chamber. Structural characterization was performed in the martensitic state at a temperature of 293 K by strain-controlled loading (0.5 mm/min) to failure. Details are described elsewhere [15, 19, 20].

Pseudoplastic materials were loaded under strain-control (0.5 mm/min) to 400 MPa at a temperature of 293 K, which was 30 K below the austenite-start-temperature (A_S) of the material. The stress limit of 400 MPa was defined in one of our former papers [19] and it was chosen because it corresponds to a stress (in the first loading cycle) where detwinning is almost completed but there is no significant plastic deformation. After reaching the maximum stress, the samples were unloaded again and subsequently heated to 393 K, which is 33 K above the austenite-finish-temperature (A_F). This allows for the phase transformation into austenite and complete shape recovery. This procedure was repeated for 15 times in order to evaluate cyclic stability of the shape memory effect. Details on this testing procedure are described elsewhere [15, 18].

Pseudoelastic materials were tested at a temperature which was 10 K above the austenite-finish temperature to ensure that the material is fully austenitic. This temperature should be far below the martensite-destruct temperature M_D or, as it is also called, martensite-dead temperature. Hence, the formation of stress-induced martensite, which is the basis for pseudoelasticity in NiTi, should hardly be impeded [22-24]. At this temperature, the samples were loaded under strain-control (0.5 mm/min) to 600 MPa and subsequently unloaded. This maximum stress level was identified in another previously published paper [15, 20] and corresponds to a stress where the stress-induced phase transformation is almost completed. Cyclic testing was also repeated 15 times in order to evaluate the cyclic stability of the pseudoelastic effect. Details on this testing procedure are described elsewhere [15, 20].

Copyright © 2013 by ASME

Downloaded From: http://proceedings.asmedigitalcollection.asme.org/ on 01/31/2016 Terms of Use: http://www.asme.org/about-asme/terms-of-use

RESULTS AND DISCUSSION

Influence of processing on structural properties and phase transformation temperatures

Understandably, one of the major goals of powder metallurgical processing methods is to produce parts with a low porosity. Figure 1 shows that the material's density strongly depends on the energy input. This energy input is a metric which summarizes several processing parameters (e.g. laser power, scanning velocity, hatch spacing, laser characteristics, …) and which can be calculated from equations given in the nomenclature and is described elsewhere more in detail [15]. Lowest densities were found at about 60 % which is in the range of the packing density of the powder [15]. It is not surprising that the density can be increased by increasing the energy input. It was found that a minimum energy input of about 100-200 J/mm³ is required to fully melt the powder and consolidate the material. Higher energy inputs do not significantly improve the density but the achieved density is higher than 99% which is very close to the theoretical density.

Obviously, the mechanical and structural behavior of a material strongly depends on the density. Figure 2 shows compression-strain curves for NiTi produced with different energy inputs. The energy inputs of between 92 and 195 J/mm³ nearly represent the upper and lower limits of the range previously identified as an optimized processing window for processing dense material while the energy input of 45 J/mm³ only allows for processing porous material. As expected, the porous material does not show high stiffness or high strength. Interestingly, the materials produced with higher energy inputs show significantly different mechanical characteristics, although their density does not differ very much. For energy inputs between 100 and 150 J/mm³ there is a scattering of achieved density of about 5% (see Figure 1). This might result in a degradation of the structural properties of the material.

We observed similar results for tensile testing of steel samples which do not significantly differ in density but which

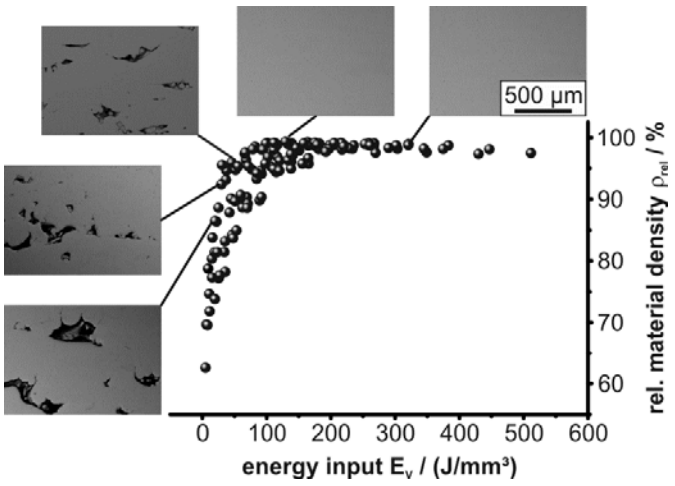

Figure 1. Influence of energy input on material's density.

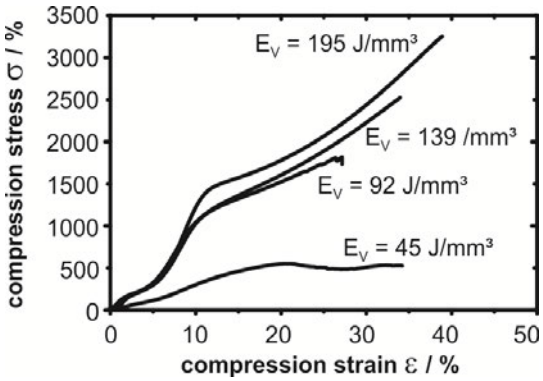

Figure 2. Influence of energy input on mechanical and structural behavior.

were produced with different energy inputs [25]. However, the samples produced with an energy input of 195 J/mm³ show very high stresses and strains at failure. The stresses are significantly higher than the fracture stresses observed by Krishna et al. [26] for similar material but produced with the AM technique LENS. Regarding the previously mentioned process window, one should adjust the energy input at the upper limit of that window to ensure optimum structural behavior. In previous works [15, 19, 20] we obtained, for compression testing of NiTi samples (produced with an optimized parameter set-up with an energy input of 195 J/mm³), that all samples show very similar and reproducible functional properties. Furthermore, their behavior is very similar compared to conventionally-processed NiTi, although the SLM samples are observed to have a slightly lower ultimate strength. However, NiTi is a functional material and typical applications do not require loading to such high stresses. Nevertheless, previous works and Figure 3 clearly attest that the stress levels are sufficient for shape memory operations.

Figure 3 shows how the impurity levels (Oxygen, Nitrogen, Carbon) develop as a result of different energy inputs during SLM. Analogous to other high temperature processing methods (melting, conventional powder metallurgy), it is assumed that there is a pick-up of impurity elements from the process chamber atmosphere, even when using an inert gas (Argon). It is well-known that low impurity content in NiTi is of great importance. All types of impurity related phases (Ti_2O, $Ti_4Ni_2O_x$, TiC, etc.) strongly affect elementary characteristics of the martensitic transformation, e.g. phase transformation temperatures, as well as the structural and functional properties of the alloy [27-29].

Interestingly, for low and high energy inputs, no increase in carbon is detected in the material. As anticipated, there is a significant increase of Nitrogen and Oxygen levels. Oxygen and Nitrogen pick-ups are shown to depend directly on the energy input. With an energy input of 100-200 J/mm³, as required to produce dense material, an Oxygen pick-up of about 0.03-0.04 wt.-%, and a Nitrogen pick-up of about 0.01-0.02 wt.-% are observed. With higher energy inputs both levels

Copyright © 2013 by ASME

Downloaded From: http://proceedings.asmedigitalcollection.asme.org/ on 01/31/2016 Terms of Use: http://www.asme.org/about-asme/terms-of-use

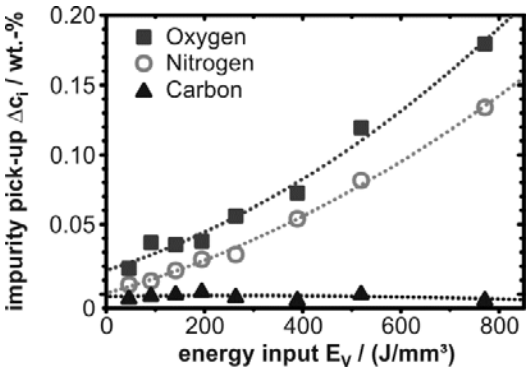

Figure 3. Influence of energy input on material's impurity contents.

increase significantly due to slower cooling time and larger melting pool dimensions. Since the powder material always contains certain impurities, it is obvious that, even when the energy input is about 100-200 J/mm³, impurity contents are acquired which are higher than the limits for medical applications (500 ppm), prescribed by the ASTM F2063-05

This shows that it is necessary to reduce the energy input to the minimal level which is required to produce dense material. Nevertheless, it can be attested that at this input of energy the impurity pick-up is relatively low in comparison to metal injection molding of NiTi [30, 31].

The impurity pick-ups can be kept to a minimum by modifying the process control. During conventional processing using the Realizer SLM 100, the inert atmosphere (Argon) is constantly filtered, recycled and recirculated in the process chamber. This method results in a constant enrichment of the Argon with Oxygen and Nitrogen, which is not filtered out. A simple method to reduce the impurity contents can be provided by constantly flooding the process chamber with fresh Argon. Figure 4 (a) shows a comparison of the impurity pick-ups for both methods. Each sample was produced with an energy input of 195 J/mm³.

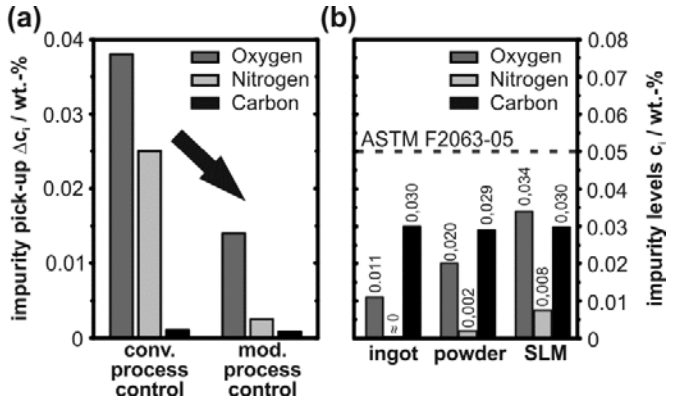

Figure 4. Comparison of impurity pick-ups for conventional and modified process control (a). Impurity contents for ingot, powder and SLM material using the modified process control (b).

By using the constant flow of fresh Argon the Oxygen pick-up can be reduced to 40 % and the Nitrogen pick-up to 15 % compared to the conventional processing set-up. By using high quality raw material, this simple modification allows for the production of high purity, medical-grade SLM NiTi which meets the requirements prescribed in the ASTM F2063-05 (see Figure 4 (b)). One might be concerned that the impurity pick-up results in a significant decrease of the transformation temperatures due to precipitation and formation of Ti-rich phases. However, it is shown that the transformation temperatures do not decrease in general. In previous works we showed that the transformation temperatures are affected by the laser treatment during SLM [15, 17, 18, 20]. We found that the transformation temperatures typically increase, even with the presence of impurity pick-ups. It is well known that laser processing can be associated with evaporation of material [32]. Titanium has a higher evaporation temperature than Nickel [33]; thus, Nickel has a higher tendency to evaporate during the laser treatment. This loss of Nickel accounts for a shift of the matrix composition to higher Titanium contents and thus the transformation temperatures increase. This result has also been reported by other authors [34, 35].

Figure 5 shows how the energy input during processing affects the transformation-start temperatures of three NiTi alloys which differ in chemical composition of initial powder. For reference, the corresponding temperatures of each powder material are also given in the figure. It is worth mentioning that all samples were produced using the conventional Argon atmosphere and flow; hence, the figure allows for a direct association with the impurity pick-ups given in Figure 3.

In general, most of the transformation-start temperatures are higher than the temperatures of the initial powder material. This indicates that the Nickel evaporation during processing compensates the impurity pick-up. Only a few Ni-rich samples (50.7 at.-%) produced with very low energy inputs exhibit transformation temperatures which are decreased. For the two other alloys, the transformation-start temperatures in samples produced with low energy inputs are very similar to temperatures in the initial powder. It is well known that the transformation temperatures of Ni-rich NiTi are particularly sensitive to impurity contents [6]. Further studies on the microstructure have to consider this decrease in detail. However, this decrease can only be observed for very low energy inputs and, as described earlier, these energy inputs do not allow for the production of dense material.

Nevertheless, a general increase of the transformation temperatures with increasing energy input can be observed although the impurity pick-ups increase, too (see Figure 3). Certainly, processing with higher energy inputs results in larger melt pool dimensions and the material is kept at elevated temperatures for longer times. Hence, more Nickel will evaporate compared to processing with low energy inputs. This Nickel loss becomes evident with an increase of the transformation temperatures. This increase is particularly evident in the Ni-rich alloy (50.7 at.-% Ni). For the Ti-rich alloy (49.7 at.-% Ni) as well as for the nearly equiatomic alloy

Copyright © 2013 by ASME

Downloaded From: http://proceedings.asmedigitalcollection.asme.org/ on 01/31/2016 Terms of Use: http://www.asme.org/about-asme/terms-of-use

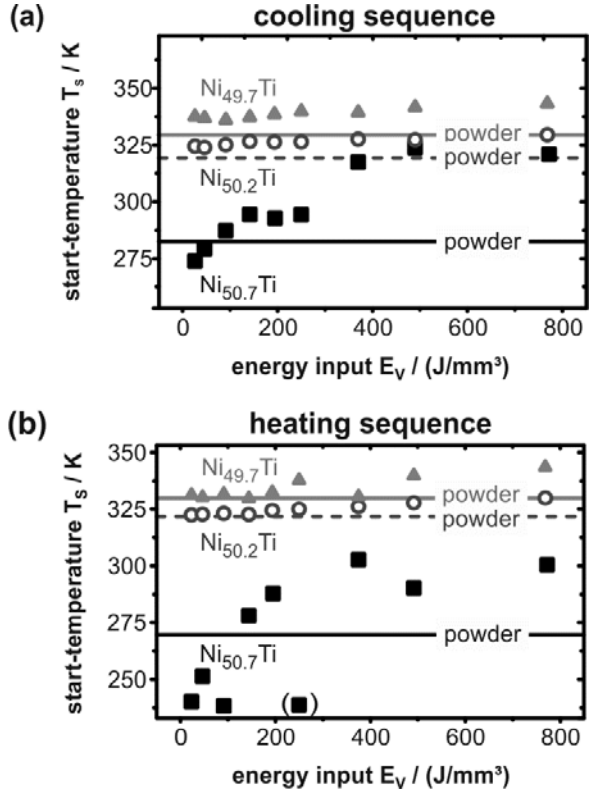

Figure 5. Influence of energy input on the transformation-start temperatures: cooling sequence (a) and heating sequence (b).

(50.2 at.-% Ni), the increase of the start temperatures is not that significant. However, there is a slight increase with increasing energy input. It is well known that when exposed to elevated temperatures Ni-rich precipitates form in Ni-rich NiTi [8, 36]. In previous works [15, 20] we showed this for SLM processing of Ni-rich NiTi. This precipitation leads to significant changes of the transformation characteristics and the transformation temperatures. It must be assumed that high energy inputs result in a higher volume of Ni-rich precipitates and in higher evaporation of Nickel, which both shift the matrix composition to higher Titanium contents. For that reason, the increase of the transformation temperatures is particularly pronounced in Ni-rich alloys.

Obviously, this work can only present a brief overview on how to optimize the process set-up for processing NiTi powders in the range of 25-75 µm. Detailed information is given elsewhere [15]. In summary, however, it is noted that an energy input of 195 J/mm³ is recommended, since dense material with sufficient structural strength can be produced and the impurity content is kept to a minimum. Nevertheless, depending on the alloy composition, a shift of the phase transformation to higher temperatures has to be expected.

Functional Properties

As shown before, NiTi can successfully be processed by SLM. However, NiTi is a functional material; hence, the functional properties of shape recovery after heating (shape memory or thermomechanical memory) and pseudoelasticity (mechanical memory) are of main interest. Thus, this paragraph presents results of functional testing of SLM NiTi for both shape memory and pseudoelasticity. As is known for conventionally processed NiTi shape memory alloys, the functional stability is limited. Generally, irreversible effects during cyclic loading are caused by the formation of dislocations. These dislocations contribute to irreversible strains 1) directly through dislocation plasticity, and 2) through the stabilization of certain martensite variants. Accordingly, there is a degradation of shape memory effect or pseudoelasticity and as a consequence an accumulation of irreversible deformation occurs.

Figure 6 shows compression testing sequences of $Ni_{50.2}Ti$ which aim to evaluate the functional stability of the shape memory effect. Each cycle starts with deformation of the material in the martensitic state. After reaching a critical stress, the detwinning of the martensite starts which accounts for large

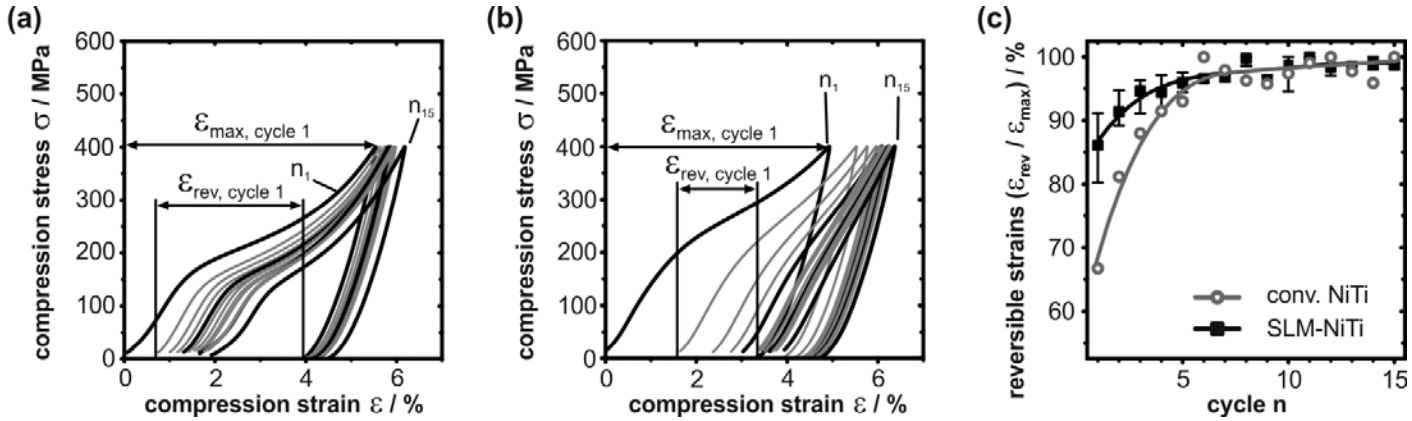

Figure 6. Evaluation of cyclic stability of shape memory: stress-strain plots of aged SLM NiTi (a) and conventional NiTi (b); proportion of reversible deformation (c).

Copyright © 2013 by ASME

Downloaded From: http://proceedings.asmedigitalcollection.asme.org/ on 01/31/2016 Terms of Use: http://www.asme.org/about-asme/terms-of-use

reversible deformation. The material was further loaded to the maximum stress (400 MPa) before being unloaded and heated up to 120°C which results in the transformation into austenite and shape recovery. This procedure was repeated 15 times. Figure 6 (a) shows SLM NiTi directly after processing (no heat treatments) whereas Figure 6 (b) shows conventionally processed NiTi (commercially purchased) with same composition. The following results can be obtained:

1. Both materials show an accumulation of irreversible deformation during cycling.
2. Highest irreversible deformation can be observed in the first cycle while they decay continuously with increasing cycles.
3. Both materials still show reversible strains in the 15th cycle.
4. It seems that the SLM material has a more stable shape recovery than the conventional material because irreversible effects appear less pronounced.

However, it is obvious that the maximum strains at 400 MPa are not exactly identical for both materials. Therefore, reversible strains cannot be compared directly. For that reason, Figure 6 (c) shows how the ratio of reversible deformation and maximum strains develops during cycling. It should be noted that the figure shows the arithmetic mean of three different SLM samples with the corresponding deviations. The previously expressed assumption of a more stable functional behavior of the SLM material is getting obvious for the first cycles. However, after cycle 6 no differences of the reversible deformation can be detected.

Figure 7 shows a similar experiment for pseudoelastic NiTi ($Ni_{50.7}Ti$). It is important to note that the SLM sample (see Figure 7 (a)) was heat treated after processing. For conventionally processed NiTi it is well known that aging treatments are necessary to support or even establish pseudoelasticity in NiTi [37]. Those aging treatments aim to precipitate Ni-rich phases of type Ni_4Ti_3. The presence of these particles results in precipitation hardening of the material and dislocation movement is impeded. Both effects contribute to an increase of the yield stress so that irreversible deformation during pseudoelastic operations is reduced. In addition, Ni_4Ti_3 particles provide nucleation sites and thus they support the martensitic transformation [38-40]. In previous works [15, 20] we showed that this well-known behavior of conventionally processed NiTi can directly be transferred to SLM NiTi. We showed that pseudoelasticity can be significantly improved by solution annealing (1225 K, 5.5 h, H_2O) followed by aging at 625 K for 24 h. Figure 7 (a) shows SLM material which was heat treated exactly in that way. Figure 7 (b) shows conventionally processed NiTi (commercially purchased) of the same composition. As described earlier, these experiments were performed 10 K above the austenite-finish temperatures of the materials, which allows for stress-induced martensitic transformation.

Both materials show characteristic pseudoelasticity but also degradation of pseudoelastic properties during cycling. While the first cycle exhibits a broad hysteresis with significant plateaus during loading and unloading, which can be referred to the stress-induced transformation, the hysteresis width decreases with increasing cycle numbers. As expected, irreversible strains accumulate during cycling. After the 15th cycle the residual strain is about 2.5 % for the conventional material and about 3.3 % for the SLM sample. Nevertheless, the SLM material clearly exhibits pseudoelastic behaviour. Especially in the first cycle, the SLM sample shows higher reversible strains than the conventional one. This can be attributd to higher maximum strains and lower plateau stress levels in the SLM material. As a consequence, stress induced transformation starts earlier.

Analogous to the experiments evaluating shape memory (see Figure 6), Figure 7 (c) considers the different strain levels by the ratio of reversible and maximum strains. This plot clearly proves that both samples behave very similar. SLM NiTi, as well as the conventionally processed NiTi, shows 95 % reversible deformation after 15 loading-unloading cycles.

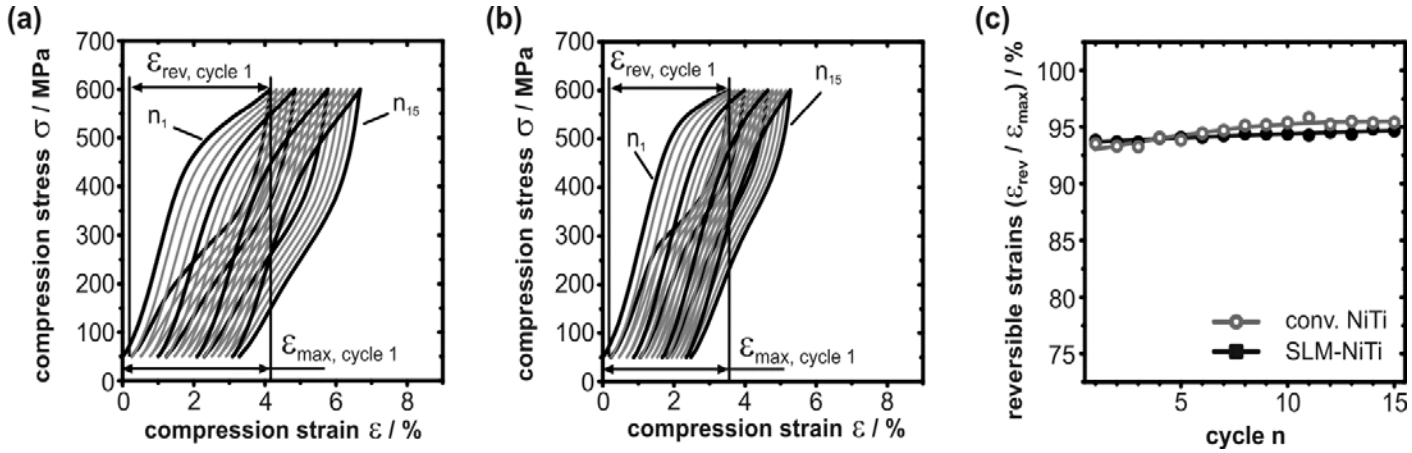

Figure 7. Evaluation of cyclic stability of pseudoelasticity: stress-strain plots of aged SLM NiTi (a) and conventional NiTi (b); proportion of reversible deformation (c).

Copyright © 2013 by ASME

Downloaded From: http://proceedings.asmedigitalcollection.asme.org/ on 01/31/2016 Terms of Use: http://www.asme.org/about-asme/terms-of-use

CONCLUSIONS

This work demonstrates the state-of-the-art of SLM processing of NiTi shape memory alloys by highlighting some of the most significant aspects of additive processing. It is shown that it is crucial to adjust the process parameter set-up in a way that dense material can processed but the impurity pick-up is kept to a minimum and the transformation temperatures are affected as little as possible. Additionally, it is shown that high quality SLM NiTi can be produced which meets the requirements for impurity contents of medical applications. Finally, this work shows that SLM NiTi exhibits distinct functional properties like shape memory and pseudoelasticity which compares favorably with the properties of conventionally processed NiTi. Thereby, this work clearly proves that AM in general, and SLM in particular, provide a promising technique to produce complex NiTi parts which may not be producible with any other method.

NOMENCLATURE

$$E_V = \frac{P_{eff}}{d_b \cdot d_l \cdot v_s} \cdot \left(2 - \frac{\Delta h}{d_t}\right) \qquad \text{for} \qquad 0 < \Delta h < d_t$$

$$E_V = \frac{P_{eff}}{d_b \cdot d_l \cdot v_s} \qquad \text{for} \qquad \Delta h \geq d_t$$

with:

E_V	= energy input / (J/mm³)
P_{eff}	= effective laser power (measured on powder bed) / W
d_b	= beam diameter / mm
d_l	= layer thickness / mm
d_t	= track width / mm
v_s	= scanning velocity / (mm/s)
Δ_h	= hatch distance / mm

The derivation of this equation is in detail explained elsewhere [15]. Optimized parameter set-up for processing NiTi powders in the range of 25-75 µm with a SLM system of type Realizer SLM100 is: $P_{eff} = 77$ W; $d_b \sim 54$ µm (TEM_{00}, $\lambda = 1076$ nm, $M^2 < 1.1$); $d_l = 50$ µm; $d_t \sim 190$ µm; $v_s = 0{,}2$ mm/s; $\Delta_h = 120$ µm. This combination results in $E_V = 195$ J/mm³.

REFERENCES

[1] Stöckel, D., 2001, "Forming Nitinol – a challenge", in: Siegert, K. (ed.): *New Developments in Forming Technology*. Frankfurt/Main, Germany: Mat-Info Werkstoff-Informationsgesellschaft mbH, pp. 119-134.

[2] Wu, M.H., 2002, "Fabrication of Nitinol Materials and Components," *Mater. Sci. Forum*, **394-395**, pp. 285-292.

[3] Wang, L.M., Liu, L.H., Yang, H., Wang, L.Y and Xiu, G.Q., 2002, "Melting and fabrication of NiTi shape-memory alloy wires," *Mater. Sci. Forum*, **394-395**, pp. 297-300.

[4] Schetky, L.McD. and Wu, M.H, 2004, "Issues in the further development of Nitinol properties and processing for medical device applications," in: Shrivastava, S. (ed.): *Medical Device Materials – Proceedings of the Materials and Processes for Medical Devices Conference*, Anaheim, CA, USA, 2003, Materials Park, OH, USA: ASM International, pp. 271-276.

[5] Sczerenie, F., 2009, extracts from an interview in Donohue, B. "Developing a good memory: Nitinol shape memory alloy," *Today's Machining World*, **3**, pp. 42-48.

[6] Frenzel, J., George, E.P., Dlouhy, A., Somsen, Ch., Wagner, M.F-X. and Eggeler, G., 2010. "Influence of Ni on Martensitic Phase Transformation in NiTi Shape Memory Alloys", *Acta Mater*. **58**, pp. 3444-3458.

[7] Großmann, C., Frenzel, J., Sampath, V., Depka, T., Oppenkowski, A. Somsen, C., Neuking, K., Theissen, W. and Eggeler, G., 2008, "Processing and Property Assessment of NiTi and NiTiCu Shape Memory Actuator Springs", *Materialwiss. Werkst.*, **39**(8), pp. 499-510.

[8] Khalil-Allafi, J., Dlouhy, A. and Eggeler, G., 2002, "Ni_4Ti_3-Precipitation during Aging of NiTi Shape Memory Alloys and its Influence on Martensitic Phase Transformations", *Acta Mat*. **50**(17), pp. 4255-4274.

[9] Biermann, D., Kahley, F., Krebs, E. and Upmeier, T., 2011, "A Study on Micro-Machining Technology for the Machining of NiTi: Five-Axis Micro-Milling and Deep-Hole Drilling," *J. Mater. Eng. Perform.*, **20(4-5)**, pp. 745-751.

[10] Wu, S.K., Lin, H.C. and Chen, C.C., 1999, "A study on the machinability of a Ti49.6Ni50.4 shape memory alloy," *Mater. Lett.*, **40**, pp. 27-30.

[11] Weinert, K. and Petzold, V., 2006, "Micromachining of NiTi Shape Memory Alloys," *Prod. Engineer. – Res. Dev.*, **13(2)**, pp. 43-46.

[12] Bellouard, Y., 2008, "Shape memory alloys for micro-systems: A review from a material research perspective," *Mat. Sci. Eng. A*, **481-482**, pp. 582-589.

[13] Worden, K., Bullough, B. and Haywood, J. (eds.), 2003, "Smart Technologies," Singapore, Singapore: *World Scientific Publishing Co. Pte. Ltd.*, p. 119.

[14] Levy, G.N., Schindel, R. and Kruth, J.-P., 2003, "Rapid Manufacturing and Rapid Tooling with Layer Manufacturing (LM) Technologies, State of the Art and Future Perspectives", *CIRP Ann.-Manuf. Techn.*, **52(2)**, pp. 589-609.

[15] Haberland, C, 2012, „Additive Verarbeitung von NiTi-Formgedächtniswerkstoffen mittels Selective Laser Melting," Ph.D. thesis Ruhr University Bochum, Aachen, Germany: Shaker Verlag.

[16] Wohlers, T., 2009, "Wohlers Report 2009. State of the Industry – Annual Worldwide Progress Report," Fort Collins, CO, USA: Wohlers Associates, Inc.

[17] Meier, H., Haberland, C., Frenzel, J. and Zarnetta, R., 2009, "Selective Laser Melting of NiTi Shape Memory Components," in Bártolo, P.J. et al. (eds.): *Innovative Developments in Design and Manufacturing – Proceedings*

Copyright © 2013 by ASME

Downloaded From: http://proceedings.asmedigitalcollection.asme.org/ on 01/31/2016 Terms of Use: http://www.asme.org/about-asme/terms-of-use

of VR@P 2009; International Conference on Advanced Research in Virtual and Rapid Prototyping, Leiria, Portugal, 2009, London, UK: CRC Press/Balkema, Taylor & Francis Group, pp 233-238.

[18] Meier, H., Haberland, C. and Frenzel, J., 2010, "Near Net Shape Processing of complex NiTi Shape Memory Components by Selective Laser Melting," in Grummon, D.S. et al. (eds.): *SMST 2010 - Proceedings of the International Conference on Shape Memory and Superelastic Technologies*, Pacific Grove, CA, USA, 2010, Materials Park, OH, USA: ASM International, pp 196-197.

[19] Meier, H., Haberland, C. and Frenzel, J., 2011, "Structural and functional Properties of NiTi Shape Memory Alloys produced by Selective Laser Melting," in Bártolo, P.J. et al. (eds.): *Innovative Developments in Virtual and Physical Prototyping – Proceedings of VR@P 2011; International Conference on Advanced Research in Virtual and Rapid Prototyping*, Leiria, Portugal, 2011, London, UK: CRC Press/Balkema, Taylor & Francis Group, pp 291-296.

[20] Haberland, C., Meier, H. and Frenzel, J., 2012, "On the Properties of Ni-rich NiTi Shape Memory Alloys produced by Selective Laser Melting," in: *Proceedings of SMASIS 2012 - Conference on Smart Materials, Adaptive Structures and Intelligent Systems*, Stone Mountain, GA, USA, 2012.

[21] Habijan, T., Haberland, C., Meier, H., Frenzel, J., Wittsiepe, J., Wuwer, C., Greulich, C., Schildhauer, T.A. and Köller, M., 2013, "The biocompatibility of dense and porous Nickel-Titanium produced by selective laser melting," *Mat. Sci. Eng. C*, **33(1)**, pp. 419-426.

[22] Otsuka K. and Wayman, C.M., 1999, "Mechanism of Shape Memory and Superelasticity", in Otsuka K. and Wayman, C.M. (eds.): *Shape Memory Materials*, University Press, Cambridge, UK, pp. 27-48.

[23] Saburi, T., 1999, "Ti-Ni Shape Memory Alloys", in Otsuka K. and Wayman, C.M. (eds.): *Shape Memory Materials*, University Press, Cambridge, UK, pp. 49-96.

[24] Gollerthan, S., Young, M.L., Baruj, A., Frenzel, J., Schmahl, W.W. and Eggeler, G., 2009, "Fracture Mechanics and Microstructure in NiTi Shape memory Alloys", *Acta Mat*. **57**, pp. 1015-1025.

[25] Meier, H. and Haberland, Ch., 2008, „Experimental Studies on Selective Laser Melting of Metallic Parts", *Materwiss. Werkst*., **39**(8), pp. 665-670.

[26] Krishna, B.V., Bose, S. and Bandyopadhyay, A., 2007, "Laser Processing of Net-Shape NiTi Shape Memory Alloy", *Metall. Mater. Trans. A*, **38**, 2007, pp. 1096-1103.

[27] Honma, T., 1987, "TiNi based shape memory alloys," in: Funakubo, H. (ed.): *Precision machinery and robotics (Volume 1) – Shape memory alloys*, New York, NY, USA: Breach Science Publishers, pp. 61-115.

[28] Johansen, K., Voggenreiter, H. and Eggeler, G., 1999, "On the effect of TIC particles in the tensile properties and on the intrinsic two way effect of NiTi shape memory alloys," *Mat. Sci. Eng. A*, **272-275**, pp. 410-414.

[29] Mentz, J., Bram, M., Buchkremer, H.P. and Stöver, D., 2006, "Improvement of mechanical properties of powder metallurgical NiTi shape memory alloys," *Adv. Eng. Mater*., **8(4)**, pp. 247-252.

[30] Bram, M., Bitzer, M., Buchkremer, H.P. and Stöver, D., 2012, "Reproducibility study of NiTi parts made by metal injection moulding," J. Mater. Eng. Perform., **21(12)**, pp. 2701-2712.

[31] Krone, L., Mentz, J., Bram, M., Buchkremer, H.P., Stöver, D., Wagner, M., Eggeler, G., Christ, D., Reese, S., Bogdanski, D., Köller, M., Esenwein, S.A., Muhr, G., Prymak, O. and Epple, M., 2005, "The potential of powder metallurgy for the fabrication of biomaterials on the basis of Nickel-Titanium: a case study with a staple showing shape memory behavior," *Adv. Eng. Mater*., **7(7)**, pp. 613-619.

[32] Majumar, J.D. and Manna, I., 2003, "Laser processing of materials," *Sadhana – Acad. P. Eng. S*, **28(3-4)**, pp. 495-562.

[33] Das, S., 2003, "Physical aspects of process control in selective laser sintering of metals," *Adv. Eng. Mater*., **5(10)**, pp. 701-711.

[34] Dudziak, S., Gieseke, M., Haferkamp, H., Barcikowski, S. and Kracht, D., 2010, "Functionality of laser-sintered shape memory micro-actuators," *Phys. Procedia*, **5**, pp. 607-615.

[35] Bormann, T., Schumacher, R., Müller, B., Mertmann, M. Michael de Wild, M., 2012, "Tailoring Selective Laser Melting Process Parameters for NiTi Implants," *J. Mater. Eng. Perform.*, **21(12)**, pp. 2519-2524.

[36] Nishida, M., Wayman, C.M. and Honma, T., 1986, "Precipitation process in near-equiatomic TiNi shape memory alloys." *Metal. Trans. A*, **17**, pp. 1505-1515.

[37] Otsuka, K. and Ren, X., 2005, "Physical metallurgy of Ti-Ni-based shape memory alloys," *Prog. Mater. Sci.*, **50**, pp. 511-678.

[38] Miyazaki, S., Imai, T., Igo, Y. and Otsuka, K., 1986, "Effect of cyclic deformation on the pseudoelasticity characteristics of Ti-Ni alloys," *Metal. Trans. A*, **17**, pp. 115-120.

[39] Gall, K. and Maier, H.J., 2002, "Cyclic deformation mechanisms in precipitated NiTi shape memory alloys," *Acta Mat*., **50**, pp. 4643-4657.

[40] Michutta, J., Somsen, C., Yawny, A., Dloughý, A. and Eggeler, G., 2006, "Elementary martensitic transformation processes in Ni-rich NiTi single crystals with Ni4Ti3 precipitates," *Acta Mat*., **54**, pp. 3525-3542.

Copyright © 2013 by ASME

Downloaded From: http://proceedings.asmedigitalcollection.asme.org/ on 01/31/2016 Terms of Use: http://www.asme.org/about-asme/terms-of-use